LETTERS
PUBLISHED ONLINE: 16 MAY 2010 | DOI: 10.1038/NPHOTON.2010.87
nature photonics

# Experimental free-space quantum teleportation

Xian-Min Jin[1†], Ji-Gang Ren[1,2†], Bin Yang[1], Zhen-Huan Yi[2], Fei Zhou[2], Xiao-Fan Xu[1], Shao-Kai Wang[2], Dong Yang[2], Yuan-Feng Hu[1], Shuo Jiang[2], Tao Yang[1], Hao Yin[1], Kai Chen[1], Cheng-Zhi Peng[2]* and Jian-Wei Pan[1,2]*

**Quantum teleportation[1] is central to the practical realization of quantum communication[2,3]. Although the first proof-of-principle demonstration was reported in 1997 by the Innsbruck[4] and Rome groups[5], long-distance teleportation has so far only been realized in fibre with lengths of hundreds of metres[6,7]. An optical free-space link is highly desirable for extending the transfer distance, because of its low atmospheric absorption for certain ranges of wavelength. By following the Rome scheme[5], which allows a full Bell-state measurement, we report free-space implementation of quantum teleportation over 16 km. An active feed-forward technique has been developed to enable real-time information transfer. An average fidelity of 89%, well beyond the classical limit of 2/3, is achieved. Our experiment has realized all of the non-local aspects of the original teleportation scheme and is equivalent to it up to a local unitary operation[5]. Our result confirms the feasibility of space-based experiments, and is an important step towards quantum-communication applications on a global scale.**

Quantum teleportation lies at the heart of a number of quantum protocols, finding particular use in quantum repeaters, quantum relays and so on, and enabling the extension of quantum communication networks to arbitrarily long distances[2,3]. Since its initial proposal by Bennett and colleagues[1], quantum teleportation has triggered significant research activity and become a focus in the field of quantum-information science. Because of negligible decoherence from the noisy environment, photonic qubits comprise one of the first physical systems to enable the realization of quantum information transfer, having the additional virtues of being easy to manipulate and capable of transmission over long distances. This led to two simultaneous successful photonic implementations of quantum teleportation—by the Innsbruck[4] and Rome groups[5]. The teleportation protocol developed by the Rome group has the advantage of allowing a full single-photon Bell-state measurement (BSM), but it is restricted in that an unknown quantum state cannot directly come from outside. Nevertheless, the Rome scheme realizes all the non-local aspects of the original teleportation scheme proposed by Bennett and colleagues[1] and is equivalent to it up to a local unitary operation[5].

These experiments have formed the solid basis for a number of demonstrations of important quantum tasks such as entanglement swapping[8], entanglement concentration[9,10], entanglement purification[11] and so on. Importantly, open-destination teleportation[12] and composite system teleportation[13] have been accomplished, making multi-party and complicated quantum networks achievable. As well as photonic realizations, teleportation has also been demonstrated between atomic qubits[14,15], and even between photonic and atomic qubits[16].

To put quantum communications applications into practice, quantum information must be transferred over much longer distances. Most earlier teleportation experiments were proof-of-principle demonstrations and lacked the ability to be implemented over large distances. Although fibre-based, long-distance teleportation has been studied experimentally[6,7], even by using state-of-the-art techniques, the maximum transmission distance is very limited as a result of huge photon losses and the decoherence effect in the optical fibre. The Geneva group[6] have realized teleportation between two laboratories, separated by 55 m and linked by means of a 2-km standard telecom fibre, and the Vienna experiment[7] achieved teleportation over a distance of 600 m through a fibre passing under the River Danube. Fortunately, in a free-space channel the photonic states are subject to harmful effects to a much lesser extent. The birefringent effect of the atmosphere is very weak, and photon absorption by the atmosphere is very small for certain wavelength regimes. Moreover, in outer space, after penetrating the aerosphere, photon loss and decoherence are negligible. Optical free-space links therefore provide the promise of much larger photon propagation distances. Although significant progress has been made in developing free-space optical links for applications in quantum communications[17–23], free-space, long-distance quantum teleportation with a full BSM and active feed-forward remains an experimental challenge.

In the present experiment, we demonstrate the transfer of a quantum state in the real scenario of public free space. The original quantum state was recovered following teleportation through a 16-km, noisy, free-space channel located on the ground. Active feed-forward technology was developed for the real-time transfer of quantum information. Importantly, the distance of 16 km is significantly greater than the effective aerosphere thickness (equivalent to 5–10 km of ground atmosphere)[20]. Such high-fidelity teleportation would pave the way for future space-based experiments, with links connecting a ground station and a satellite, or two ground stations with a satellite between acting as a relay; this has the potential for enabling quantum-communication applications on a global scale in the near future.

A schematic layout of the experimental set-up is shown in Fig. 1a. This set-up (following the Rome scheme) has advantages over many previous experiments[4,6,7] in that it avoids synchronization between single photon states with ultrashort coherence times over large distances, and prevents the very low detection rates associated with the simultaneous detection of three photons. In our experiment, Charlie and Alice are located at Badaling in Beijing (40° 21′ 38″ N, 115° 56′ 22″ E, 550 m altitude) at the teleportation site, and Bob is located at Huailai in Hebei province (40° 22′ 02″ N, 115° 45′ 09″ E, 500 m altitude) at the receiver site. The straight-line distance between the two stations is ~16 km. At the

[1]Hefei National Laboratory for Physical Sciences at Microscale and Department of Modern Physics, University of Science and Technology of China, Hefei, Anhui, 230026, PR China, [2]Physics Department, Tsinghua University, Beijing 100084, PR China; †These authors contributed equally to this work.
*e-mail: pcz@mail.tsinghua.edu.cn; pan@ustc.edu.cn



© 2010 Macmillan Publishers Limited. All rights reserved.

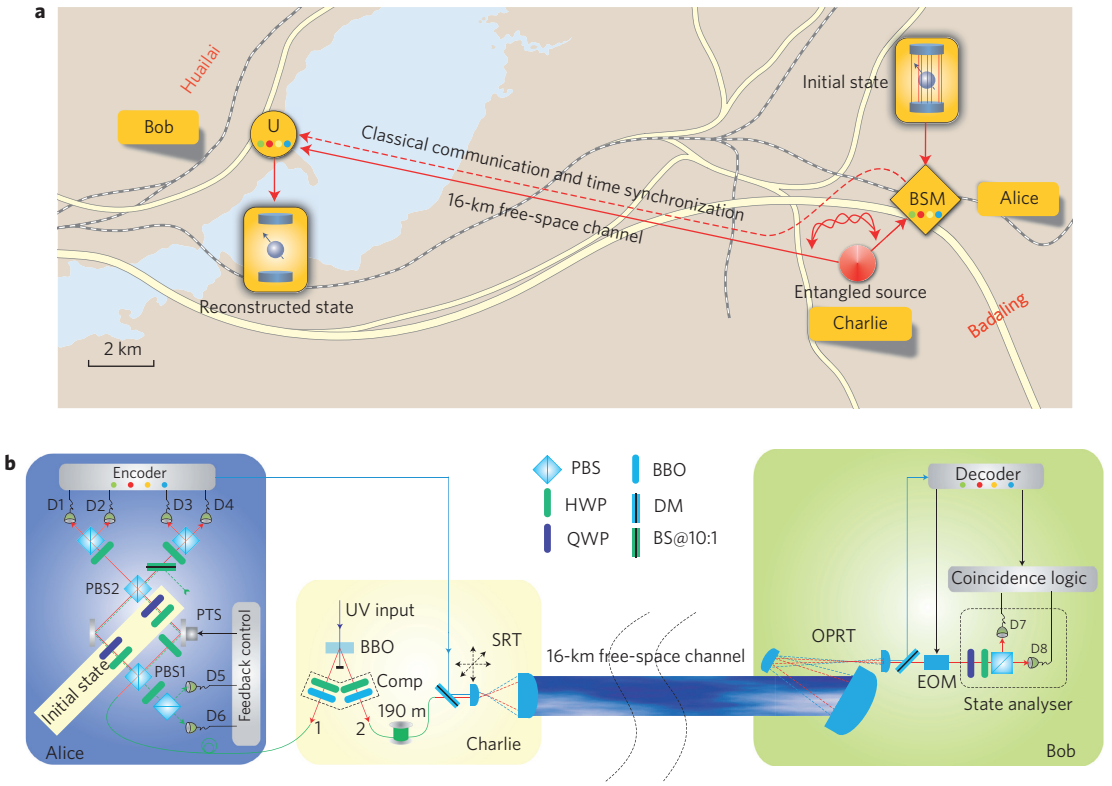


**Figure 1 | Experimental quantum teleportation in free space. a**, A birds-eye view of the 16-km free-space quantum teleportation experiment. Charlie sends photon 1 to Alice for BSM. Classical information, including the results of the BSM and the signal for time synchronization, is sent through the free-space channel with photon 2, to Bob, before decoding and triggering of the corresponding unitary transformation. **b**, Sketch of the experimental system. The phase-locking laser (green dashed) is injected into the interferometer to probe phase drift for feedback control on the PTS. The results of the BSM and the time information are modulated to laser pulses (638 nm, blue line) with Hamming code by Encoder, before combining with photon 2 (red line) using a DM. They are then sent together to Bob's site by the SRT. Once received by the OPRT, they are split with another DM, and analysed by Decoder to apply the corresponding unitary operation on photon 2 through the EOM, and to subject the time synchronization signal to coincidence logic for coincidence measurement.

teleportation site (see Fig. 1b), a semiconductor, blue laser beam (power 34.5 mW, waist 100 μm, central wavelength 405 nm) is incident on a 2-mm β-barium-borate (BBO) crystal to generate entangled photon pairs at 810 nm by means of type-II spontaneous parametric down-conversion (SPDC)[24]. The down-converted extraordinary and ordinary photons have different propagating velocities, and will travel along different paths inside the crystal due to the birefringent effect of the BBO crystal. The resulting walk-off effects are then compensated by a combination of a half-wave plate (HWP) and an additional 1-mm BBO crystal in each arm. Collecting with single-mode fibre (SMF), we locally observed ~110,000 $s^{-1}$ single photons in each arm of the source, and obtained 32,600 polarization-entangled photon pairs per second. The visibility of the polarization correlations was observed to be ~95% for the horizontal/vertical (H/V) basis and 89% for the $+45^{\circ}/-45^{\circ}$ basis, substantiating the high quality of our entangled photon source. To achieve complete BSM, we followed the teleportation protocol developed in the Rome experiment[5]. In the experiment, the polarization-entangled photon source was aligned to produce the singlet state

$$|\Psi^{-}\rangle_{1p2p} = \frac{1}{\sqrt{2}}\left(|H\rangle_{1p}|V\rangle_{2p} - |V\rangle_{1p}|H\rangle_{2p}\right) \quad (1)$$

where $|H\rangle_{1p}(|V\rangle_{1p})$ denotes that photon 1 is in the horizontal (vertical) polarization state. The same applied for photon 2.

Freely propagating photon 2 passes through public free space across towns, roads, factories and the Guanting Lake, and eventually arrives at Bob's station. To optimize the transmission efficiency and improve the stability of the free-space channel, we designed two types of telescopes to act as optical transmitting and receiving antennas, one split-type refracting telescope (SRT) for Charlie, and one off-axis parabolic reflecting telescope (OPRT) for Bob. The SRT was constructed to be portable by separating the ocular and object lens and by not having a draw tube. The ocular lens ($f = 0.05$ m), built into a micrometre-resolution positioning stage to enable tri-axial movement, and a long-focus object lens (focus length 2.372 m, diameter 0.2 m) were used to achieve precise angle adjustment of the laser beam with steps of 0.42 μrad. Position adjustment at Bob's site was achieved with a precision of 7 mm per step for matching the optical spot displacement. The spot diameter at the receiving site ranged from 0.4 to 1 m, depending on weather conditions. The OPRT had a large aperture (diameter 0.4 m), good stability (weight ~1,000 kg and stability 0.3 μrad $h^{-1}$) and a high transmission efficiency of >80% at a wavelength of 800 nm. We were able to adjust the signal beam to propagate out from the middle of the OPRT tube, so that a breadboard carrying the optical components of the receiving system could be fitted into the middle part. With this configuration the stability of the OPRT could be greatly enhanced by improving the balance of the telescope tube.

To prepare the unknown quantum state to be teleported, Charlie first allows photon 1 to pass through a polarization beamsplitter (PBS1), which acts as the operation $|H\rangle_{1p} \Rightarrow |H\rangle_{1p}|R\rangle_{1w}$ and $|V\rangle_{1p} \Rightarrow |V\rangle_{1p}|L\rangle_{1w}$, where $|R\rangle_{1w}(|L\rangle_{1w})$ denotes that photon 1 follows the right (left) path. Subscript 'p' denotes the polarization



© 2010 Macmillan Publishers Limited. All rights reserved.

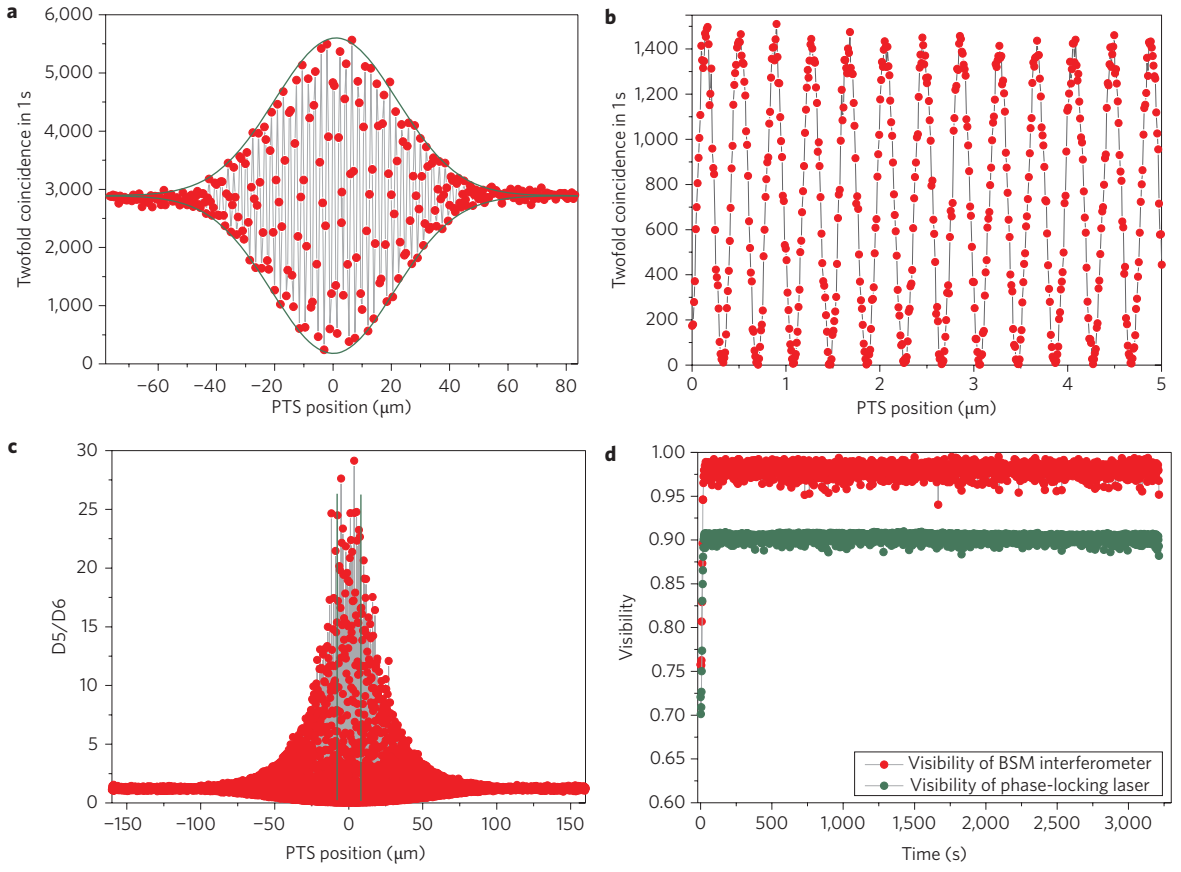


**Figure 2 | Experimental data for characterizing the BSM interferometer. a**, Searching for perfect temporal overlap of two spatial modes of photon 1. As a signature of perfect temporal overlap, the high-visibility interference envelope is observed by measuring the twofold coincidence between D1 and photon 2. **b**, Performing a fine scan with a PTS at the middle of the interference envelope. A high visibility of 99.2% is obtained after further optimization, implying that accurate spatial and temporal overlap is achieved for the two modes of photon 1. **c**, With application of the phase-locking laser, the detected count ratios of D5 to D6 change as a function of PTS position. **d**, Stabilization of the phase of the BSM interferometer. It can be actively stabilized with a precision better than $\lambda/52$ with feedback control. The visibility of the BSM interferometer (red symbols) holds at a level of 98% as long as the visibility of the phase-locking laser (green symbols) is locked at 90%.

mode, and subscript 'w' denotes the path mode, indicating which path the photon follows (left or right). The whole state can thus be expressed as

$$|\Psi^-\rangle_{1w1p2p} = \frac{1}{\sqrt{2}}\left(|R\rangle_{1w}|H\rangle_{1p}|V\rangle_{2p} - e^{i\phi}|L\rangle_{1w}|V\rangle_{1p}|H\rangle_{2p}\right) \quad (2)$$

By inserting a zero-order HWP in the right path to switch H to V, one can initialize the polarization states of photon 1 in both spatial modes to the vertical polarization. Phase $\phi$ can be fixed at zero by active feedback control of the interferometer (see Methods). The two photons will therefore be maximally entangled in the spatial modes of photon 1 and polarization modes of photon 2:

$$|\Psi^-\rangle_{1w2p} = |V\rangle_{1p} \otimes \frac{1}{\sqrt{2}}\left(|R\rangle_{1w}|V\rangle_{2p} - |L\rangle_{1w}|H\rangle_{2p}\right) \quad (3)$$

In the phase-locked interferometer, a combination of zero-order HWP and quarter-wave plate (QWP) are then used to create the unknown polarization state to be teleported, $|\Psi\rangle_{1p} = \alpha|H\rangle_{1p} + \beta|V\rangle_{1p}$, where $\alpha$ and $\beta$ are two complex numbers satisfying $|\alpha|^2 + |\beta|^2 = 1$. We define four Bell states as $|\Psi^\pm\rangle_{1w1p} = (|R\rangle_{1w}|V\rangle_{1p} \pm |L\rangle_{1w}|H\rangle_{1p})/\sqrt{2}$ and $|\Phi^\pm\rangle_{1w1p} = (|R\rangle_{1w}|H\rangle_{1p} \pm |L\rangle_{1w}|V\rangle_{1p})/\sqrt{2}$. The combinative state of the three qubits can then be rewritten as

$$\begin{aligned}|\Psi\rangle_{1p1w2p} &= |\Psi\rangle_{1p} \otimes |\Psi^-\rangle_{1w2p} \\ &= \frac{1}{2}(|\Psi^-\rangle_{1p1w} + |\Phi^-\rangle_{1p1w}\hat{\sigma}_x - |\Phi^+\rangle_{1p1w}i\hat{\sigma}_y \\ &\quad - |\Psi^+\rangle_{1p1w}\hat{\sigma}_z)|\Psi\rangle_{2p}\end{aligned} \quad (4)$$

This implies that a joint BSM at Alice's site can projects photon 2 into one of four corresponding states in equation (4). The complete BSM can be achieved by overlapping the two spatial modes of photon 1 on a second polarizing beamsplitter PBS2 and performing a further polarization analysis along the $\pm 45^\circ$ polarization basis (that is, the $|\pm 45^\circ\rangle = (|H\rangle \pm |V\rangle)/\sqrt{2}$ basis) in the two output modes of PBS2 (ref. 5). Bob can thus deterministically recover the initial states $|\Psi\rangle_{1p}$ by applying a corresponding unitary transformation on photon 2 with regard to the BSM results (see Methods).

Successful implementation of quantum teleportation requires a high-visibility BSM interferometer, which directly affects the final teleportation fidelity. To accomplish high-quality BSM, it is necessary to ensure that the two output modes of photon 1 have perfect spatial and temporal overlap behind the PBS2. Experimentally, the spatial modes of photon 1 are well-defined due to the use of SMF. Interference filters with a bandwidth of 8 nm are set in front of



© 2010 Macmillan Publishers Limited. All rights reserved.

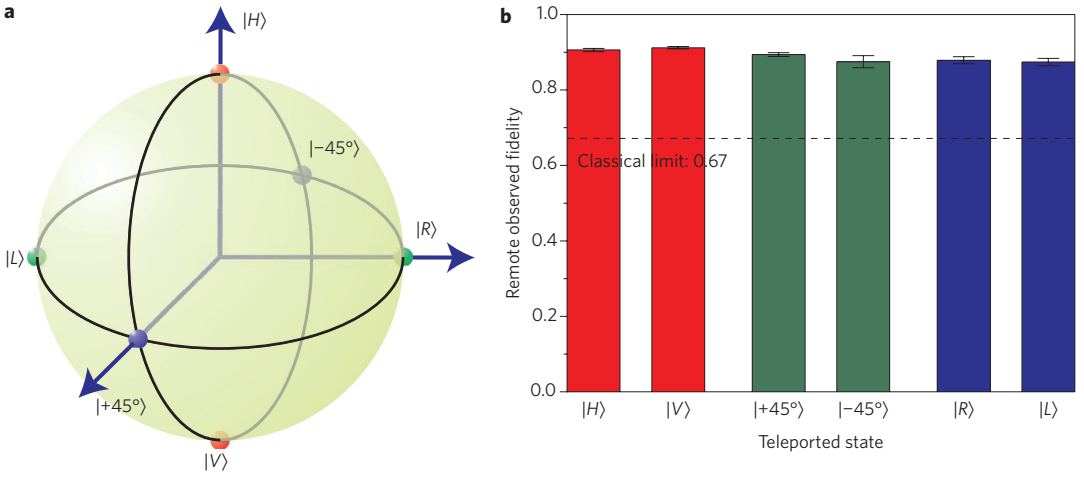


**Figure 3 | Experimental results of teleportation of six universal states. a**, Bloch sphere representation of the six initial states to be teleported. **b**, Observed fidelities, denoted by different colours for different initial states, significantly exceed the classical limit of 2/3. Error bars are given by Poissonian statistics.

the SMF to provide the required spectral modes. A prism is built in a precision linear stage (not shown in Fig. 1) to achieve the rough temporal overlap for the two spatial modes of photon 1. The prism is further controlled by a piezoceramics translation stage (PTS) to achieve fine adjustment of the position of the prism. To optimize the temporal overlap, a polarizer (oriented at $+45^\circ$) is inserted before the left input mode of PBS1 and all wave plates in the BSM interferometer are set to $0^\circ$, corresponding to an injection of the $|\Phi^+\rangle_{1w1p}$ state. The twofold coincidence between D1 and photon 2 would thus yield an interference envelope. As is shown in Fig. 2a, we scanned over a large scale with a step size of 500 nm to search the interference envelope. At the middle position of the envelope, an interference visibility of 93.7% was observed, implying that high-quality BSM is achieved. To further optimize the visibility of the BSM interferometer, we prepared the initial state behind the PBS1 in $|+45^\circ\rangle$ and perform a fine scan with a step size of 10 nm by measuring twofold coincidence between D1 and photon 2. As shown in Fig. 2b, a final optimized visibility of 99.2% was obtained.

To prove the universality of the teleportation set-up, we selected linear polarization states $|H\rangle$, $|V\rangle$, $|+45^\circ\rangle$ and $|-45^\circ\rangle$ and circular polarization states $|R\rangle = (|H\rangle + i|V\rangle)/\sqrt{2}$ and $|L\rangle = (|H\rangle - i|V\rangle)/\sqrt{2}$ as the initial states to be teleported (see Fig. 3a). A good evaluation of the performance of our experiment is given by measuring teleportation fidelity, defined as $F = \mathrm{Tr}(\hat{\rho}|\Psi\rangle_{1p1p}\langle\Psi|)$, where $|\Psi\rangle_{1p}$ is the original state and $\hat{\rho}$ is the density matrix of the teleported state. The fidelity can be reformulated by Pauli matrices and a density matrix as

$$\begin{aligned} F &= \mathrm{Tr}(\hat{\rho}|\Psi\rangle_{1p1p}\langle\Psi|) \\ &= \mathrm{Tr}(\hat{\rho}(|\alpha|^2(\hat{\mathrm{I}}+\hat{\sigma}_z) + \alpha\beta^*(\hat{\sigma}_x + i\hat{\sigma}_y) + \beta\alpha^*(\hat{\sigma}_x - i\hat{\sigma}_y) \\ &\quad + |\beta|^2(\hat{\mathrm{I}}-\hat{\sigma}_z))/2 \end{aligned} \tag{5}$$

This implies that one can evaluate the fidelity for the teleported state by performing only local measurements of $\hat{\sigma}_x$, $\hat{\sigma}_y$ and $\hat{\sigma}_z$. In our case, the fidelities for the six teleported states are $F_{|H\rangle} = \mathrm{Tr}(\hat{\rho}(\hat{\mathrm{I}}+\hat{\sigma}_z))/2$, $F_{|V\rangle} = \mathrm{Tr}(\hat{\rho}(\hat{\mathrm{I}}-\hat{\sigma}_z))/2$, $F_{|+45^\circ\rangle} = \mathrm{Tr}(\hat{\rho}(\hat{\mathrm{I}}+\hat{\sigma}_x))/2$, $F_{|-45^\circ\rangle} = \mathrm{Tr}(\hat{\rho}(\hat{\mathrm{I}}-\hat{\sigma}_x))/2$, $F_{|R\rangle} = \mathrm{Tr}(\hat{\rho}(\hat{\mathrm{I}}+\hat{\sigma}_y))/2$ and $F_{|L\rangle} = \mathrm{Tr}(\hat{\rho}(\hat{\mathrm{I}}-\hat{\sigma}_y))/2$, respectively. At Bob's site, a state analyser comprising a PBS, an HWP and a QWP is used to project the teleported state to $|\Psi\rangle_{1p}$ and its orthogonal state $|\Psi\rangle_{1p}^{\perp}$. Experimentally, to obtain the real teleportation fidelity one has to eliminate the biased effect caused by the different detection efficiencies of D7 and D8 (see Methods and Table 1). Thanks to the high coincidence rate during the time period 19:30–22:00 (see Methods), ~50–1,850 events per minute are observed, depending on weather conditions, and an integration time of 5 min is therefore sufficient for each teleportation measurement. As is plotted in Fig. 3b, the experimental results for teleportation fidelity for different initial states range from 87% to 91%, with an overall average fidelity of 89%. All the measured fidelities are well beyond the classical limit of 2/3 (ref. 25), supporting the demonstration of successful high-quality teleportation.

Note that we have not set a significant spatial separation for the locations of Alice and Charlie in the present demonstration, which is also the case in the earlier demonstrations reported in refs 6 and 7. We plan to implement such a feature in the near future, with additional optical transmitting and receiving modules, and develop relevant optical spot stabilizing techniques. As already mentioned in the introduction, our approach, adopted from that of the Rome group, is restricted in that an unknown quantum state cannot directly come from outside. It is because of this restriction that the name 'remote state preparation' is sometimes applied to the Rome teleportation scheme. As noted in ref. 5, however, this restriction can in principle be overcome through locally swapping an unknown arbitrary state from outside to the polarization degree of freedom with a series of controlled-NOT gates. The demonstration here is therefore equivalent to the original teleportation scheme only up to a local unitary operation.

In the present experiment, we have followed the Rome scheme to achieve quantum teleportation in free space over a distance of 16 km. This is the longest reported distance over which photonic teleportation has been achieved to date, more than 20 times longer than the previous implementation for a fibre channel[6,7]. Various techniques have been developed for accomplishing this goal, including real-time feedback control of the high-stability interferometer for single-photon BSM, active feed-forward manipulation of the single-photon state for reconstruction of the initial teleported qubit, novel design of telescopes tailored for teleportation experiments, and so on. The excellent quality of the recovered state with an average fidelity better than 89% is thereby obtained. The transmission loss of the overall system is generally at a level of 30 dB. If we use a large-aperture telescope and high-accuracy ATP (acquisition, tracking and pointing) techniques, the transmission loss between low-Earth-orbit satellites and ground stations can be well controlled to this level by theoretical estimation. Our



© 2010 Macmillan Publishers Limited. All rights reserved.

**Table 1 | Experimental measurement for teleportation fidelities.**

| Initial states | $\|H\rangle$ | $\|V\rangle$ | $\|+45°\rangle$ | $\|-45°\rangle$ | $\|R\rangle$ | $\|L\rangle$ |
|---|---|---|---|---|---|---|
| $\|\Psi\rangle_{1p}$ (D7) | 2,936 | 4,939 | 2,027 | 213 | 591 | 631 |
| $\|\Psi\rangle_{1p}^{\perp}$ (D8) | 225 | 391 | 276 | 30 | 83 | 103 |
| $\|\Psi\rangle_{1p}$ (D8) | 3,232 | 5,125 | 1,279 | 152 | 553 | 300 |
| $\|\Psi\rangle_{1p}^{\perp}$ (D7) | 458 | 605 | 131 | 22 | 74 | 38 |
| Fidelities | 0.906(4) | 0.912(3) | 0.894(5) | 0.875(16) | 0.879(9) | 0.874(11) |

experiment therefore confirms the feasibility of teleportation-based quantum communications for satellite–ground applications. In the meantime, our set-up allows fast realization of teleportation, mainly due to the high count rates from the compact entangled photon source and the intrinsic virtue of the scheme from ref. 5. Although in our experiment successful teleportation occurs probabilistically with post-selection, it can still be used as a high-quality quantum relay as shown in ref. 6. If combined with quantum memory, long-distance quantum teleportation and related quantum information applications, a quantum communication network may come within reach of current technology on a global scale.

## Methods

**Locking interferometer by active feedback control.** A challenge for our experiment is that the single-photon interferometer for BSM requires long-term sub-wavelength stability. Most earlier experiments used so-called passive stabilization by protecting the interferometer from unwanted mechanical vibration and temperature drift. However, such a method can only keep the phase stable over timescales of minutes and is not suitable for achieving long-term stability. We have made a crucial improvement by actively stabilizing the BSM interferometer with an additional phase-locking laser. As is shown in Fig. 1b, labelled in green with a dashed line, the phase-locking laser (wavelength 808 nm), $+45°$ polarized, is coupled into the BSM interferometer along the reverse-propagating direction of photon 1. At the output of PBS1, we analyse the polarization for the $+45°/-45°$ basis and send the results to the feedback control system (Fig. 2c), where an active control algorithm gives a feedback signal to the PTS to set the phase shift of the BSM interferometer to zero. The instability can be suppressed within $\lambda/52$ (see Fig. 2d for an illustration).

**Active feed-forward for complete teleportation.** Note that an active teleportation experiment was first performed in ref. 26 by the Rome group. To perform the corresponding active unitary transformations on the teleported qubits at Bob's site, in this experiment we built in high-precision time synchronization between the sender and the receiver. With the assistance of high-frequency laser pulse modulation, the time information and the results of BSM were encoded to a string of pulses. Hamming code was used to overcome the fluctuation in the receiving efficiency induced by atmospheric turbulence. Photon 2 was delayed by 190 m of SMF and coupled with the synchronization laser by means of a dichromatic mirror (DM, T808R633), then sent to Bob together with the SRT. The magnification factor of the SRT was chosen to be $\times 47$. At Bob's station, the mixed beam is received by the giant telescope OPRT, separated by an additional DM. the synchronization laser beam is detected with a photon receiver and analysed with a self-designed decoder. The received information includes both the results of BSM for unitary transformation and signal for time synchronization. The accuracy of time synchronization that was achieved was better than 1 ns. The BSM results were used to trigger a high-voltage module to drive fast electro-optical modulators (EOM) able to realize corresponding unitary transformation on photon 2. For example, if the output of BSM is $|\Phi^-\rangle_{1p1w}$, the EOM will perform the unitary transformation $\sigma_x$ on photon 2 to reconstruct the teleported state $|\Psi\rangle_{1p}$ by applying a high voltage of 0.83 kV. For the remaining outputs, the EOM will work by analogy, to apply $\hat{1}$ for $|\Psi^-\rangle_{1p1w}$, $i\hat{\sigma}_y$ for $|\Phi^+\rangle_{1p1w}$ and $\hat{\sigma}_z$ for $|\Psi^+\rangle_{1p1w}$, respectively.

**Fidelity measurement.** In the experiment, the state analyser at Bob's site projects the states $|\Psi\rangle_{1p}$ and $|\Psi\rangle_{1p}^{\perp}$ into the modes D7 and D8, respectively. Then, within a certain period of time, the twofold coincidence counts between photon 1 and D7 (D8), denoted $C_7$ ($C_8$), are proportional to $N\eta_C F\eta_7$ ($N\eta_C(1-F)\eta_8$), where $N$ is the total number of photon pairs generated, $\eta_C$ denotes the transmission efficiency of photon 2 in the free-space channel, $\eta_7$ ($\eta_8$) denotes the overall detection efficiency of detector D7 (D8) (including the collection and detection efficiencies), and $F$ is the teleportation fidelity. Because, in general, $\eta_7 \neq \eta_8$, it is impossible to deduce the precise value of $F$ from the observed $C_7$ and $C_8$. To obtain the real teleportation fidelity, we swapped the projection measurement with rotating wave plates in the state analyser to project the states $|\Psi\rangle_{1p}$ and $|\Psi\rangle_{1p}^{\perp}$ into the modes D8 and D7, respectively. While considering the drift in transmission efficiency, within the same integration time the twofold coincidence counts between photon 1 and D7 (D8), denoted by $C_7'$ ($C_8'$), are proportional to $N\eta_C'(1-F)\eta_7$ ($N\eta_C' F\eta_8$), where $\eta_C'$ denotes the new channel transmission efficiency. In this way it is possible to eliminate the influence of the biased detection efficiency and the transmission efficiency drift and obtain the real teleportation fidelity with $F = 1/(1+\sqrt{C_7'C_8/C_7C_8'})$.

**Estimation of transmission efficiency.** Air pollution and flow are the two main factors influencing optical transmittance quality in the free-space channel. Optical link efficiency between the SRT and the OPRT was observed to be between 14 and 31 dB and varied depending on the weather conditions. The total loss was estimated to be composed of ~9.5–21.5 dB from atmospheric losses, 1.5 dB from attenuation in the components of the two telescopes, and ~3–8 dB arising from geometric losses (where the beam area is larger than the aperture of the OPRT). At Bob's side, the loss of coupling in the multimode fibre is 5.2 dB, and the attenuation introduced by optical elements including filters and pockels cells is ~1.9 dB. At Alice's side, the components in the BSM interferometer account for 1.9 dB. The coupling loss in the SMF is 5.9 dB for two uses. The 190-m SMF causes an additional loss of 0.3 dB. The loss for the overall system therefore ranges from 29.2 to 46.2 dB. At the time of our particular experiment, the total loss was ~32 dB. Every month there are ~10 days for testing when the weather conditions are such that there is a sufficiently high atmospheric visibility of greater than 20 km. We find that the time period between 19:30 and 22:00 is best for experiments due to the low absorption, reduced air convection and affordable background noise at those times. After 5:00, the background count will normally rise from 1,300 to 10,000 $s^{-1}$ within several minutes, and experiments should be halted because of the low signal-to-noise ratio. To confirm that the qubit could survive after experiencing an extremely challenging noisy environment, polarization analysers using a bright signal laser were performed. A fidelity of 97.3% for the $+45°/-45°$ basis and 97.8% for the H/V basis were achieved before the main teleportation experiment.

Received 9 June 2009; accepted 16 March 2010; published online 16 May 2010

## References


1. Bennett, C. H. *et al.* Teleporting an unknown quantum state via dual classic and Einstein–Podolsky–Rosen channels. *Phys. Rev. Lett.* **70,** 1895–1899 (1993).
2. Briegel, H.-J., Dür, W., Cirac, J. I. & Zoller, P. Quantum repeaters: the role of imperfect local operations in quantum communication. *Phys. Rev. Lett.* **81,** 5932–5935 (1998).
3. Gisin, N., Ribordy, G., Tittel, W. & Zbinden, H. Quantum cryptography. *Rev. Mod. Phys.* **74,** 145–195 (2002).
4. Bouwmeester, D. *et al.* Experimental quantum teleportation. *Nature* **390,** 575–579 (1997).
5. Boschi, D., Branca, S., De Martini, F., Hardy, L. & Popescu, S. Experimental realization of teleporting an unknown pure quantum state via dual classical Einstein–Podolsky–Rosen channels. *Phys. Rev. Lett.* **80,** 1121–1125 (1998).
6. Marcikic, I., De Riedmatten, H., Tittel, W., Zbinden, H. & Gisin, N. Long-distance teleportation of qubits at telecommunication wavelengths. *Nature* **421,** 509–513 (2003).
7. Ursin, R. *et al.* Quantum teleportation across the Danube. *Nature* **430,** 849–849 (2004).
8. Pan, J.-W., Bouwmeester, D., Weinfurter, H. & Zeilinger, A. Experimental entanglement swapping: entangling photons that never interacted. *Phys. Rev. Lett.* **80,** 3891–3894 (1998).
9. Yamamoto, T., Koashi, M., Özdemir, S. K. & Imoto, N. Experimental extraction of an entangled photon pair from two identically decohered pairs. *Nature* **421,** 343–346 (2003).
10. Zhao, Z., Yang, T., Chen, Y.-A., Zhang, A.-N. & Pan, J.-W. Experimental realization of entanglement concentration and a quantum repeater. *Phys. Rev. Lett.* **90,** 207901 (2003).
11. Pan, J.-W., Gasparoni, S., Ursin, R., Weihs, G. & Zeilinger, A. Experimental entanglement purification of arbitrary unknown states. *Nature* **423,** 417–422 (2003).
12. Zhao, Z., Chen, Y.-A., Zhang, A.-N., Yang, T., Briegel, H. -J. & Pan, J.-W. Experimental demonstration of five-photon entanglement and open-destination teleportation. *Nature* **430,** 54–58 (2004).




© 2010 Macmillan Publishers Limited. All rights reserved.

13. Zhang, Q. *et al.* Experimental quantum teleportation of a two-qubit composite system. *Nature Phys.* **2,** 678–682 (2006).
14. Riebe, M. *et al.* Deterministic quantum teleportation with atoms. *Nature* **429,** 734–737 (2004).
15. Barrett, M. D. *et al.* Deterministic quantum teleportation of atomic qubits. *Nature* **429,** 737–739 (2004).
16. Chen, Y.-A. *et al.* Memory-built-in quantum teleportation with photonic and atomic qubits. *Nature Phys.* **4,** 103–107 (2008).
17. Hughes, R. J. *et al.* Practical free-space quantum key distribution over 10 km in daylight and at night. *New J. Phys.* **4,** 43.1–43.14 (2002).
18. Kurtsiefer, C. *et al.* Quantum cryptography: a step towards global key distribution. *Nature* **419,** 450 (2002).
19. Aspelmeyer, M. *et al.* Long-distance free-space distribution of quantum entanglement. *Science* **301,** 621–623 (2003).
20. Peng, C.-Z. *et al.* Experimental free-space distribution of entangled photon pairs over a noisy ground atmosphere of 13 km: towards satellite-based global quantum communication. *Phys. Rev. Lett.* **94,** 150501 (2005).
21. Ursin, R. *et al.* Free-space distribution of entanglement and single photons over 144 km. *Nature Phys.* **3,** 481–486 (2007).
22. Villoresi, P. *et al.* Experimental verification of the feasibility of a quantum channel between space and Earth. *New J. Phys.* **10,** 033038 (2008).
23. Fedrizzi, A. *et al.* High-fidelity transmission of entanglement over a high-loss free-space channel. *Nature Phys.* **5,** 389–392 (2009).
24. Kwiat, P. G. *et al.* New high-intensity source of polarization-entangled photon pairs. *Phys. Rev. Lett.* **75,** 4337–4341 (1995).
25. Massar, S. & Popescu, S. Optimal extraction of information from finite quantum ensembles. *Phys. Rev. Lett.* **74,** 1259–1263 (1995).
26. Giacomini, S., Sciarrino, F., Lombardi, E. & De Martini, F. Active teleportation of a quantum bit. *Phys. Rev. A* **66,** 030302(R) (2002).

## Acknowledgements

This research, leading to the results reported here, was supported by the Chinese Academy of Sciences, the National Fundamental Research Program of China under grant no. 2006CB921900, and the National Natural Science Foundation of China.

## Author contributions

J.-W.P. and C.-Z.P. supervised the project overall. J.-W.P., C.-Z.P. and H.Y. designed the experiment. X.-M.J., J.-G.R., B.Y., Z.-H.Y., F.Z., X.-F.X., S.-K.W., S.J., T.Y. and C.-Z.P. performed the experiment. D.Y. and Y.-F.H. designed the electric devices. X.-M.J., J.-G.R., K.C. and J.-W.P. analysed the data. X.-M.J., K.C., C.-Z.P. and J.-W.P. wrote the paper.

## Additional information

The authors declare no competing financial interests. Reprints and permission information is available online at http://npg.nature.com/reprintsandpermissions/. Correspondence and requests for materials should be addressed to C.-Z.P. and J.-W.P.



© 2010 Macmillan Publishers Limited. All rights reserved.